Research Journal of Applied Sciences, Engineering and Technology 7(6): 1172-1182, 2014
DOI:10.19026/rjaset.7.377
ISSN: 2040-7459; e-ISSN: 2040-7467

Submitted: March 07, 2013 Accepted: April 05, 2013 Published: February 15, 2014

Research Article

Second Order Effect in Unbraced Steel Frames at Ultimate State

Nazzal S. Armouti
Department of Civil Engineering University of Jordan, Amman 11942, Jordan, Tel.: 0799476699

Abstract: Second order effect is evaluated for unbraced frames at ultimate state. As a case study, an unbraced one bay frame is evaluated using first order elastic, second order elastic, first order plastic and second order plastic analyses. Second order plastic analysis is based on proposed procedures using magnification factor as its basis. These procedures take the effect of formation of plastic hinges and in turn, the softening of the frame on the critical load (buckling load) of the frame into consideration. It has been found by second order plastic analysis that frame strength dramatically deteriorates after formation of the second plastic hinge. While first order plastic analysis puts the strength on the ascending branch, second order analysis puts the strength on the descending branch of load-deformation curve regardless of the level of axial load in the system. It has also been found that while full mechanism failure develops under low levels of axial load, it cannot develop under moderate and high levels of axial loads. Furthermore, it has been found that the strength deteriorate rapidly after formation of the second plastic hinge leads to early collapse before the development of full failure mechanism. The codes are challenged to produce practical procedures for second order effect to account for structure behavior at ultimate state.

Keywords: Frame buckling, plastic hinge, plastification sequence, plastic magnification factor

INTRODUCTION

Plastic analysis and design is permitted by design codes as a mean of more realistic behavior leading to more savings by utilizing the member capacity to its fullest extent. However, design codes do not explicitly address detailed rules on methods of design, especially, the consideration of second order effect associated with plastic analysis and design. Trends in current and future methods in the analysis and design of steel frames are summarized by Trahair (2012). Classical plastic analysis may be found in Beedle (1958), while modern techniques in plasticity and plastic analysis are found in Chen and Sohal (1995), Chen and Han (1988) and Wong (2009). Various developments in methods of second order plastic analysis are given by Alvarenga and Silveira, (2009a, b), Mesic (2007), Chan and Zhou (2004) and Bi *et al*. (2004).

As it is known, second order analysis results in amplification of forces and moments which may be evaluated by explicit second order analysis (P-D effect), or by means of the well recognized magnification factors applied to the first order forces and moments as obtained from first order analysis. These magnification factors are recognized in steel codes such as AISC (American Institute of Steel Construction) (2010) and ACI (American Concrete Institute) (2011).

The magnification factors given in design codes are calculated as function of Euler buckling loads assuming structures to remain elastic, therefore, they are elastic buckling loads.

Evaluation of second order effect in plastic analysis is not addressed in the design codes, i.e., it is not clear how to evaluate the magnification factors in association with plastic analysis. In plastic analysis and design, structures are considered safe and functional up the level of mechanism formation. If second order effect has to be considered in this case, formation of plastic hinges has to be taken into consideration.

As plastic hinges form, they reduce redundancy of structures and at the same time, soften them. This action, definitely, reduces the buckling capacity of structures and consequently, increases the magnification factors of the first order forces and moments. This reduction in buckling capacity and increase in magnification factors could adversely affect the behavior and economics of design using plastic methods.

In view of the above discussion, this study explores the effect of plastic hinge formation in the structure on the magnification of the first order plastic analysis using a one bay steel frame as a case study. The effect of axial load is also included as a varying parameter in the columns as shown later.

CASE STUDY

In order to explore the effect of plastification of structures on second order effect (magnification of first order analysis), a one bay steel frame is considered as a case study for this purpose. The frame is subjected to two main forces that cause mechanisms to develop,

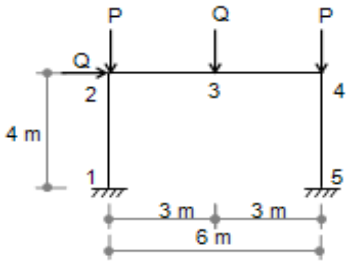

Fig. 1: Frame layout

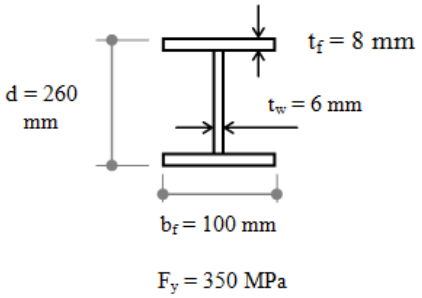

Fig. 2: Cross section

namely, lateral force, Q and vertical force, Q, as shown in Fig. 1. In addition, the frame is subjected to an axial force, P, in each vertical member of the frame, as also shown in Fig. 1, to serve as a varying parameter for the intended parametric study. For reference purposes, the different locations of potential plastic hinge locations in the frame are designated from node 1 to node 5 as also shown in Fig. 1.

A constant cross section is selected for the frame from AISC manual (AISC, 2010). This section is W-shape (W10×17 inch × lb/ft) which is equivalent to (W 250×25 mm×kg/m) in SI units. The dimensions of this section are shown in Fig. 2, which will be used for calculations of all section properties. A common steel yield stress is selected for the material, F_y = 350 MPa.

The frame capacity is calculated according to four various procedures, namely:

- First order elastic analysis procedures
- Second order elastic analysis procedures
- First order plastic analysis procedures
- Second order plastic analysis procedures, as suggest by this study. The second order plastic analysis procedures are based on consideration of the sequence of formation of plastic hinges on the stability of the frame (Frame Buckling Load).

In addition, an incremental analysis is performed to track the resistance of the frame as each of the plastic hinges form up to failure. This sequence of plastification analysis is performed including the axial load as a varying parameter given as percentage of the axial yield load of the column, P_y. Accordingly, the

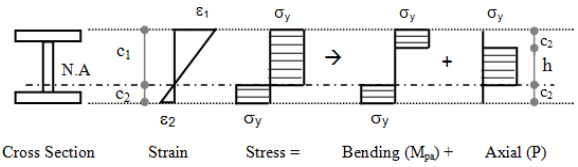

Fig. 3: Plastic section modulus and plastic moment

Table 1: Section dimensions and properties

h	t_w	b_f	t_f	A	P_y	Z_x	M_p
mm	mm	mm	mm	mm^2	kN	mm^3	kN.m
260	6	100	8	3064	1072	290904	101.816

parameter variation includes four analysis methods and six levels of axial loads in the column, namely, 10, 20, 30, 40, 60 and 75% respectively. Note that the parameter variation includes 20% as the border of interaction equations given by AISC for elastic capacity of frame-columns; and the 75% which is the limit of axial load level allowed by AISC for columns to be included in frames under plastic design criterion.

It should be pointed out that the steel section selected is compact. In addition, the frame is assumed to be fully braced and, therefore, the full capacities of the sections are utilized.

Section properties and capacities: The section properties are calculated based on the dimensions given in Fig. 2. In this study, the plastic moment and section modulus are denoted M_p and Z_x respectively. The plastic moment capacity and section modulus in presence of axial load is considered and denoted M_{pa} and Z_{xa}, respectively. For clarity, the section modulus and plastic moment calculations are based on the strain and stress distributions shown in Fig. 3.

The calculated section properties are shown in Table 1 and 2.

First order elastic frame capacity: To find the factored internal forces and moment, structural analysis is performed for the frame under external loads, Q = 10 kN. The resulting reactions and internal moments are shown in Fig. 4. Note that the maximum moment in the frame takes place at right reaction (node 5) which is related to the external loads Q by the factor, α_Q, such that:

$$Q = \alpha_Q M_{max}$$

$$\alpha_Q = 10 / 14.767 = 0.6772$$

The first order elastic capacity of the frame is considered in this study for comparison purposes. This capacity is based on AISC interaction equations for frame-columns which take the form:

$$\text{For } \frac{P_u}{\phi_c P_n} \geq 0.2 \rightarrow \frac{P_u}{\phi_c P_n} + \frac{8}{9}\left(\frac{M_u}{\phi_b M_n}\right) \leq 1$$

Table 2: Plastic moment and section modulus in presence of axial load

P_u/P_y	Ratio	0	0.05	0.1	0.2	0.3	0.4	0.6	0.75
Z_{xa}	mm^3	290904	289926	286992	275257	255698	228316	155573	98113
M_{pa}	kN.m	101.816	101.474	100.447	96.340	89.494	79.910	54.450	34.339
M_{pa}/M_p	Ratio	1	0.997	0.987	0.946	0.879	0.785	0.535	0.337

Table 3: First order elastic frame load capacity at various axial load intensities

P_u/P_y	Ratio	0.1	0.2	0.3	0.4	0.6	0.75
M_u	kN.m	86.544	80.180	68.726	57.272	34.363	17.182
Q_u	kN	57.742	53.496	45.854	38.212	22.927	11.464

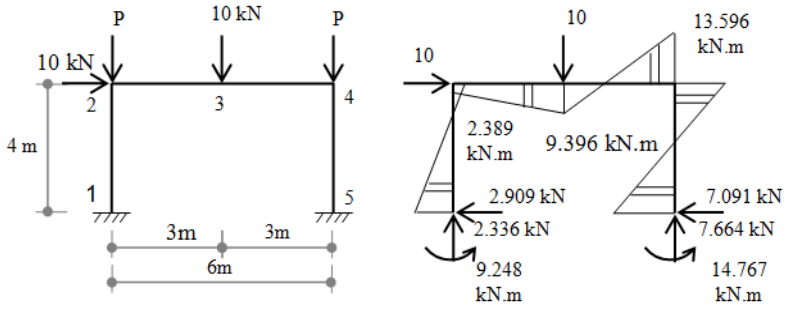

Fig. 4: Bending moment diagram

$$\text{For } P_u/\phi_c<0.2 \rightarrow \frac{P_u}{2\phi_c P_n}+\left(\frac{M_u}{\phi_b M_n}\right)\le 1$$

where ϕ_c and ϕ_b are the strength reduction factors for compression and flexure respectively. P_n and M_n are the nominal section capacities which are taken for compact fully braced sections as $P_n = F_y A = P_y$ and $M_n = F_y Z_x$. Accordingly:

$P_n = F_y A = 350\ (3064) = 1072400$ N (1072 kN)
$M_n = F_y Z_x = 350\ (290904) = 101816400$ N.m (101.816 kN.m)
$\phi_c = \phi_b = 0.9$

For each ratio of P_u/P_y, the above equations yield the ultimate moment capacity which can, in turn, yield the ultimate load capacity, Q_u, using the above mentioned factor, α_Q. For example, if a ratio of (P_u/P_y = 0.2) is used, these procedures yield:

$$\text{For } \frac{P_u}{\phi_c P_n} \ge 0.2 \rightarrow \frac{P_u}{\phi_c P_n}+\frac{8}{9}\left(\frac{M_u}{\phi_b M_n}\right)\le 1 \rightarrow$$

$$\frac{0.2}{0.9}+\frac{8}{9}\left(\frac{M_u}{0.9(101.816)}\right)\le 1 \rightarrow M_u = 80.180 \text{ kN.m}$$

Hence,

$$Q_u = \alpha_Q M_u = 0.6772\ (80.180) = 53.496 \text{ kN}$$

Similar procedures yield the load capacity for the various ratios of P_u/P_y as shown in Table 3.

Second order elastic frame capacity: The second order elastic frame capacity is based on AISC interaction equations for beam-columns taking into consideration the magnification factor for sway members (unbraced), B2. If B2 is taken into consideration, the interaction equations for beam-column may be put in the following form:

$$\text{For } \frac{P_u}{\phi_c P_n} \ge 0.2 \rightarrow \frac{P_u}{\phi_c P_n}+\frac{8}{9}\left(\frac{B2.M_u}{\phi_b M_n}\right)\le 1$$

$$\text{For } \frac{P_u}{\phi_c P_n} < 0.2 \rightarrow \frac{P_u}{2\phi_c P_n}+\left(\frac{B2.M_u}{\phi_b M_n}\right)\le 1$$

where, B2, is the magnification factor for unbraced frames and is given in the following form:

$$B2 = \frac{1}{1-\frac{\Sigma P_u}{\Sigma P_e}} \ge 1$$

where,
ΣP_u = Summation of all vertical loads in the frame
= Summation of Q and 2P in our case
ΣP_e = Summation of all critical loads of all frame columns

which is found by frame stability analysis in this study

The exact critical load of the frame may be found by the second order slope deflection method (stability function procedure). However, this method may be very closely approximated by utilization of the geometric

Table 4: Second order elastic frame load capacity at various axial load intensities

P_u/P_y	Ratio	0.1	0.2	0.3	0.4	0.6	0.75
M_u	kN.m	83.250	74.078	60.880	48.554	26.517	12.278
Q_u	kN	55.545	49.425	40.619	32.395	17.692	8.192

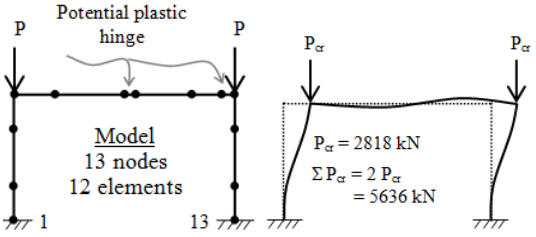

(a) Frame discretization (b) Frame buckling load and buckling shape

Fig. 5: Elastic buckling load of frame by geometric stiffness method

stiffness matrix in conjunction with the stiffness matrix. In this study, the critical load is found by this approach of geometric stiffness method which, in fact, is form of Finite Element Analysis (Chen and Lui, 1987).

If the right hand rule sign convention for forces and moments is used, the element stiffness matrix, $[k_m]$ and the geometric stiffness matrix, $[k_{Gm}]$, take the following form

$$[k_m]=\frac{EI}{L^3}\begin{bmatrix} 12 & 6L & -12 & 6L \\ 6L & 4L^2 & -6L & 2L^2 \\ -12 & -6L & 12 & -6L \\ 6L & 2L^2 & -6L & 4L^2 \end{bmatrix}, [k_{Gm}]=\frac{P}{30L}\begin{bmatrix} 36 & 3L & -36 & 3L \\ 3L & 4L^2 & -3L & -L^2 \\ -36 & -3L & 36 & -3L \\ 3L & -L^2 & -3L & 4L^2 \end{bmatrix}$$

Assembly of the global stiffness and geometric stiffness matrices; and standard solution of eigenvalue problem leads to obtaining the buckling loads and their buckling shapes of the system.

Figure 5 shows the modeling of the frame utilized in this study which is descetized into 13 nodes and 12 elements. Very short elements are introduced at the location of the potential plastic hinges in order to take the formation of plastic hinges into consideration for later analysis as shown in Fig. 5a. The resulting first buckling load of the frame and its buckling shape is shown in Fig. 5b. As can be seen, the critical load of one column, P_{cr} = 2818 kN.

Accordingly, the magnification factor, B2, may now be calculated. If the load ratio of P_u/P_y = 0.2 is considered for example, B2 is calculated as follows:

$$P_u = 0.2\ P_y = 0.2\ (1072) = 214.4\ \text{kN}$$

$$B2 = \frac{1}{1-\frac{\Sigma P_u}{\Sigma P_e}} = \frac{1}{1-\frac{214.4}{2818}} = 1.082 > 1 \text{ ok.}$$

The ultimate load capacity may now be calculated using the interaction equation as follows:

$$\text{For } \frac{P_u}{\phi_c P_n} \geq 0.2 \rightarrow \frac{P_u}{\phi_c P_n}+\frac{8}{9}\left(\frac{B2\,.M_u}{\phi_b M_n}\right) \leq 1 \rightarrow$$

$$\frac{0.2}{0.9}+\frac{8}{9}\left(\frac{1.082\,M_u}{0.9\,(101.816)}\right) \leq 1 \rightarrow M_u = 74.107\ \text{kN.m}$$

Hence, $Q_u = \alpha_Q M_u = 0.6772\ (74.107) = 49.425$ kN

Similar procedures yield the load capacity for the various ratios of P_u/P_y as shown in Table 4.

First order plastic frame capacity (mechanism method): The first order plastic analysis can be performed using lower bound or upper bound theorem (Beedle, 1958; Chen and Sohal, 1995; Wong, 2009). In this study, the upper bound theorem is used to find the ultimate load (mechanism load). The frame used in this analysis is three times statically indeterminate; and hence has a number of redundant forces, R = 3. It also has a number of potential locations for plastic hinges, N = 5. The number of independent mechanism, m, can be found accordingly as:

$$m = N–R = 5–3 = 2$$

The total number of mechanisms that can occur in this frame are 3 mechanisms, two independent, namely, beam mechanism and sway mechanisms. If these two mechanisms are combined, they result in a third combined mechanism. These three mechanisms are shown graphically in Fig. 6 which will be investigated to yield the true mechanism that produces the correct ultimate load as the smallest of the three.

It is assumed that the reader is familiar with mechanism analysis, therefore, the analysis will be performed accordingly. Notice that in presence of the axial load, the moment capacity of the beam becomes M_{pa} as explained previously. In hindsight, it can be observed from Fig. 4b that the loads produced by Q are fraction of Q and hence are considered negligible in comparison with the high loads added to the columns, P, for parametric study. Therefore, only the column section capacity will be affected by the added axial loads, P and will be assigned the values of the parameter variation as a total in the section, i.e., 0.1, 0.2, 0.3, 0.4, 0.6 and 0.75 of P_y.

If the power produced by external forces is denoted, $\bar{P}$ and the internal dissipation is denoted, $\bar{D}$, ultimate load capacity, Q_m, for each mechanism is calculated. For illustration purpose, consider the case of P_u/P_y, = 0.2 which yields the following:

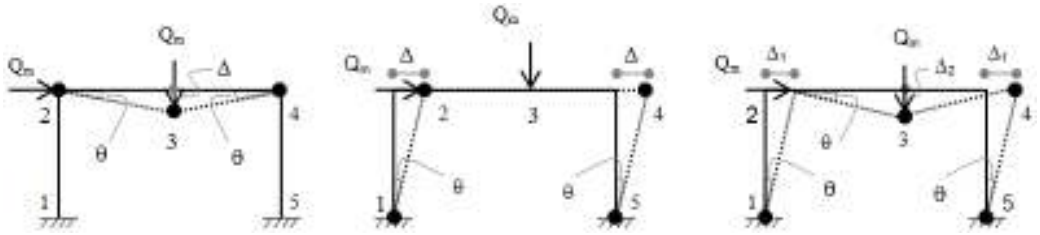

(a) Beam mechanism (b) Sway mechanism (c) Combined mechanism

Fig. 6: Types of possible failure mechanisms in frame

Table 5: First order frame true ultimate load capacity at various axial load intensities

P_u/P_y	Ratio	0.1	0.2	0.3	0.4	0.6	0.75
M_{pa}	kN.m	100.447	96.340	89.494	79.910	54.450	34.339
Q_m	kN	86.49	84.142	80.230	74.754	54.450	34.340
Q_u	kN	77.840	75.728	72.207	67.278	49.006	30.906
Controlling Mechanism		Combined mechanism				Sway mechanism	

- **Beam mechanism:** Refer to Fig. 6a for notation and recall that $M_{pa} = 0.946\ M_p$ (Table 2), hence

$\bar{P} \geq \bar{D}$
$Q_m.\Delta = M_{p2}(\theta) + M_{p3}(2\theta) + M_{p4}(\theta)$
$Q_m.(3\theta) = M_{pa}(\theta) + M_p(2\theta) + M_{pa}(\theta) = M_{pa}(4.114\theta)$ or, $Q_m = 1.371\ M_{pa}$

- **Sway mechanism:** Refer to Fig. 6b for notation and recall that $M_{pa} = 0.946\ M_p$ (Table 2), hence:

$\bar{P} \geq \bar{D}$
$Q_m.\Delta = M_{p1}(\theta) + M_{p2}(\theta) + M_{p4}(\theta) + M_{p5}(\theta)$
$Q_m.(4\theta) = M_{pa}(\theta) + M_{pa}(\theta) + M_{pa}(\theta) + M_{pa}(\theta)$
or, $Q_m = 1.0\ M_{pa}$

- **Combined mechanism:** Refer to Fig. 6c for notation and recall that $M_{pa} = 0.946\ M_p$ (Table 2), hence:

$\bar{P} \geq \bar{D}$
$Q_m.\Delta_1 + Q_m.\Delta_2 = M_{p1}(\theta) + M_{p3}(2\theta) + M_{p4}(2\theta) + M_{p5}(\theta)$
$Q_m.(4\theta) + Q_m.(3\theta) = M_{pa}(\theta) + M_p(2\theta) + M_{pa}(2\theta) + M_{pa}(\theta)$
or, $Q_m = 0.873\ M_{pa}$

Therefore, the true ultimate load equals to $Q_m = 0.873\ M_{pa}$ and is controlled by the combined mechanism. Accordingly:

$Q_m = 0.873\ M_{pa} = 0.873\ (96.34) = 84.143$ kN
$Q_u = \phi\ Q_m = 0.9\ (84.143) = 75.728$

Similar procedures yield the true ultimate load capacity for the various ratios of P_u/P_y as shown in Table 5.

First order sequence of plastification and resistance: In order to evaluate the second order effect during plastification and in order to compare results with first order plastic analysis, it will be required to find the frame resistance at the formation of each plastic hinge in the frame up to the failure state, i.e., at mechanism. Therefore, the resistance of the frame at the formation of each plastic hinge is evaluated by incremental analysis as usually done in plastic analysis methods.

As an example of calculations, the case of $P_u/P_y = 0.2$ is considered. The tracking of resistance of the frame at the formation of each plastic hinge is worked out in stages as follows:

- **First plastic hinge:** Inspection of the bending moment diagram shown in Fig. 4 indicates that the maximum moment takes place in right support (node 5) and therefore, becomes the first plastic hinge to form. The load that is required to form the first plastic hinge, Q_1, at the right support is obtained by proportionality of loading. The plastic moment at ($P_u/P_y = 0.2$) is obtained from Table 2 as, $M_{pa} = 96.34$ kN.m. By proportionality of loading, the bending moment diagram is obtained for the first plastic hinge as shown in Fig. 7a, hence:

$Q_1 = 65.239$ kN
$Q_{1u} = \phi\ Q_1 = 0.9\ (65.240) = 58.715$ kN

- **Second plastic hinge:** To reach the second plastic hinge, an incremental loading is required. The incremental load shall be applied as additional increment, ΔQ_1, to the structure after formation of the first plastic hinge. Since the plastic hinge cannot take any additional loading, the new structure becomes as shown in Fig. 7b. After drawing an initial bending moment diagram and by

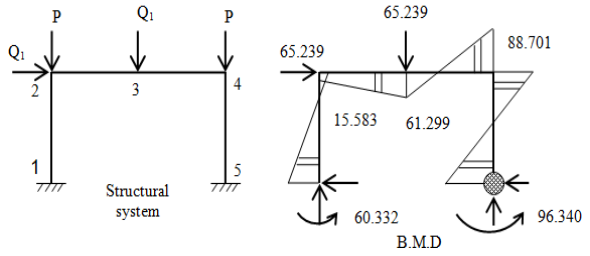

(a) First plastic hinge state

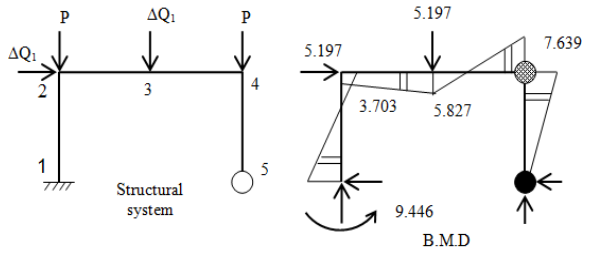

(b) Incremental load ΔQ1, to develop second plastic hinge state

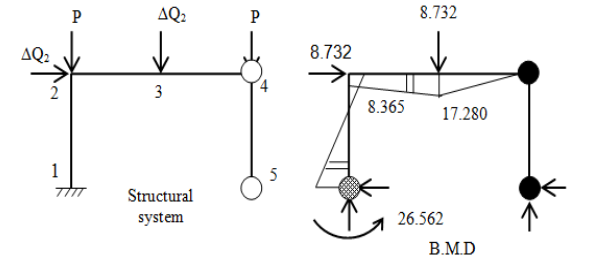

(c) Incremental load ΔQ_2, to develop third plastic hinge state

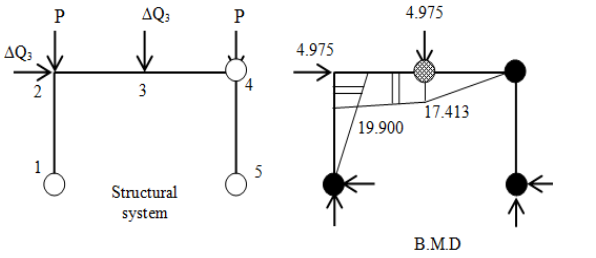

(d) Incremental load ΔQ_3, to develop fourth plastic hinge state

Fig. 7: Incremental bending moment diagrams (Tension side, Units in kN, m)

inspection, the second plastic hinge is found to form at the right joint of the frame (joint 4). The incremental bending moment diagram to achieve this state is shown in Fig. 7b, hence:

$\Delta Q_1, = 5.197$ kN
$Q_2 = Q_1 + \Delta Q_1, = 65.239 + 5.197 = 70.436$ kN
$Q_{2u} = \phi\ Q_2 = 0.9\ (70.436) = 63.392$ kN

- **Third plastic hinge:** To reach the third plastic hinge, an incremental loading is required as done before. The incremental load shall be applied as additional increment, ΔQ_2, to the structure after formation of the second plastic hinge. Since the plastic hinge cannot take any additional loading, the new structure becomes as shown in Fig. 7c. After drawing an initial bending moment diagram and by inspection, the third plastic hinge is found to form at the left support of the frame (joint 1). The incremental bending moment diagram to achieve this state is shown in Fig. 7c, hence:

$\Delta Q_2, = 8.732$ kN
$Q_3 = Q_2 + \Delta Q_2, = 70.436 + 8.732 = 79.168$ kN
$Q_{3u} = \phi\ Q_3 = 0.9\ (79.168) = 71.251$ kN

- **Fourth plastic hinge:** The fourth plastic hinge is the last plastic hinge. The load will be of course the true mechanism load. For procedure checking purposes, the incremental procedure is used to reach the fourth plastic hinge as done before. The incremental load shall be applied as additional increment, ΔQ_3, to the structure after formation of the third plastic hinge. Since the plastic hinge cannot take any additional loading, the new structure becomes as shown in Fig. 7d. After drawing an initial bending moment diagram and by inspection, the fourth plastic hinge is found to form at the beam midspan (joint 3). The incremental bending moment diagram to achieve this state is shown in Fig. 7d. Noting that the plastic moment capacity of the beam is given as $M_p = 101.816$ as given in Table 1, the required load becomes

$\Delta Q_3, = 4.975$ kN
$Q_4 = Q_3 + \Delta Q_3, = 79.168 + 4.975 = 84.143$ kN
$Q_{4u} = \phi\ Q_4 = 0.9\ (84.143) = 75.729$ kN

Notice that the incremental load procedures yield an ultimate load, $Q_{4u} = 84.143$, which coincides with the ultimate load, $Q_m = 84.143$, obtained by mechanism method procedures used earlier.

The incremental load procedures are performed for the other cases of P_u/P_y ratios required in this parametric study. Table 6 shows the nominal load capacity at the formation of each plastic hinge, Q_i, whereas, Table 7 shows the ultimate load capacity at the formation of each plastic hinge, ϕQ_i.

Second order plastic frame capacity: The second order plastic frame capacity is found by using the magnification factor, B2, as give by AISC. In this study, B2, will be based on the frame buckling load

Table 6: Nominal load capacity at sequence of plastification at various axial load intensities, Q_i

P_u/P_y	Ratio	0.1	0.2	0.3	0.4	0.6	0.75
Q_1	kN	68.020	65.239	60.603	54.114	36.870	23.254
Q_2	kN	73.440	70.436	65.431	58.424	39.810	25.106
Q_3	kN	82.540	79.168	73.543	65.667	44.750	28.219
$Q_4 = Q_m$	kN	86.490	84.142	80.230	74.754	54.450	34.340
Controlling Mechanism		Combined mechanism				Sway mechanism	

Table 7: Ultimate load capacity at sequence of plastification at various axial load intensities, $Q_{iu} = \phi Q_i$, $\phi = 0.9$

P_u/P_y	Ratio	0.1	0.2	0.3	0.4	0.6	0.75
Q_{1u}	kN	61.221	58.717	54.545	48.704	33.187	20.929
Q_{2u}	kN	66.102	63.399	58.895	52.588	35.833	22.598
Q_{3u}	kN	74.293	71.255	66.192	59.104	40.273	25.398
$Q_{4u} = \phi Q_m$	kN	77.840	75.728	72.207	67.278	49.006	30.906
Controlling Mechanism		Combined mechanism				Sway mechanism	

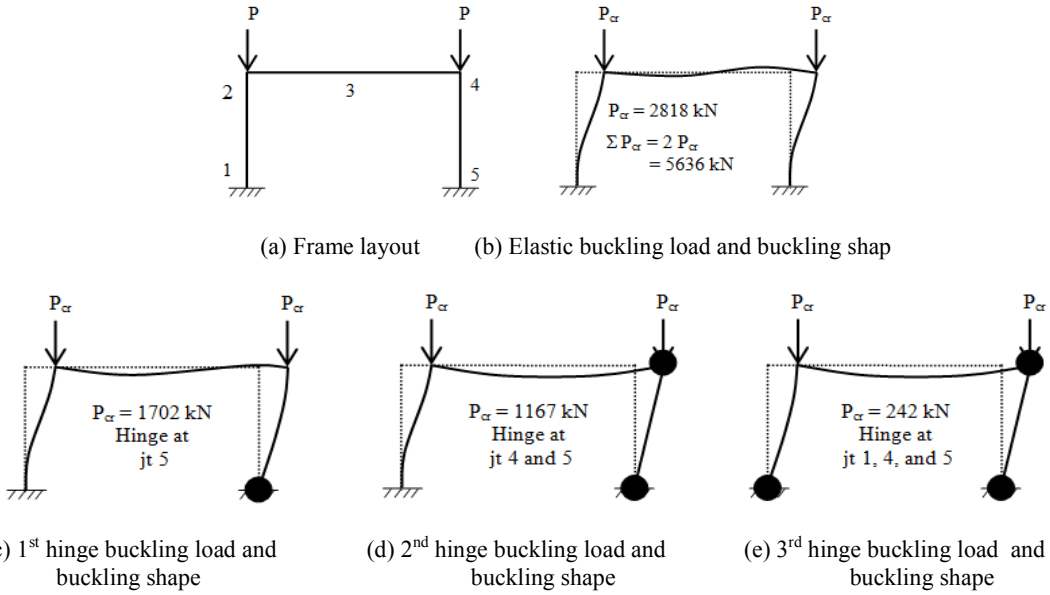

(a) Frame layout (b) Elastic buckling load and buckling shap

(c) 1st hinge buckling load and buckling shape (d) 2nd hinge buckling load and buckling shape (e) 3rd hinge buckling load and buckling shape

Fig. 8: Buckling load at formation of plastic hinges by geometric stiffness method

taking plastic hinge formation into account. The frame capacity may be reached before the full development of true mechanism due to second order effect; therefore, it becomes necessary to evaluate the resistance load at the formation of each plastic hinge.

In order to do so, it will be necessary to calculate the frame buckling load at the formation of each plastic hinge and evaluate the magnification factor, B2, accordingly. This magnification factor, calculated on the basis of plastic hinge formation, will be referred to in this study as the plastic magnification factor, B2.

Therefore, the second order ultimate capacity will be calculated by multiplying the first order ultimate load capacity by the plastic magnification factor.

The analysis performed to find the sequence of plastification outlined in the previous section indicates that in both controlling mechanisms, i.e., the sway mechanism and the combined mechanism, the sequence of plastification is the same for the first three plastic hinges, namely, at joint 5, then 4 and then 1. The final plastic hinge will form at joint 2 for the sway mechanism and at joint 3 for the combined mechanism. Therefore, the buckling for the frame in each mechanism will be the same for the formation of the first three plastic hinges. The buckling load after the formation of the last plastic hinge will be zero since the frame has reached its mechanism with total stiffness of zero.

Using the same model for buckling given in Fig. 5 and introducing the plastic hinges in the model as they form, the frame buckling load and its mode shape is found as each plastic hinge forms as shown in Fig. 8.

In the following sections, the plastic magnification factor will be calculated accordingly. For demonstration purpose, the load ratio of $P_u/P_y = 0.2$ is considered as an example. In this case, the ultimate load, P_u is given as:

$$P_u = 0.2\ P_y = 0.2\ (1072) = 214.4\ \text{kN}$$

B2: Just before formation of first plastic hinge: The elastic buckling load is already found in previous sections for the evaluation of the elastic magnification

Table 8: Plastic magnification factor, B2, at sequence of plastification at various axial load intensities

P_u/P_y	0.1	0.2	0.3	0.4	0.6	0.75
Elastic	1.040	1.082	1.129	1.180	1.296	1.399
1st plastic hinge	1.067	1.144	1.233	1.337	1.608	1.896
2nd plastic hinge	1.101	1.225	1.381	1.581	2.229	3.218
3rd plastic hinge	1.796	8.794	---	---	---	---
4th plastic hinge	---	---	---	---	---	---
Controlling mechanism	Combined mechanism				Sway mechanism	

factor, B2, which is also shown in Fig. 8b and repeated here for completeness of presentation as:

P_{cr} = 2818 kN
B2 = 1.082

B2: At formation of first plastic hinge: The buckling load just after the formation of the first plastic hinge is shown in Fig. 8c, which leads to the following:

P_{cr} = 1702 kN

$$B2 = \frac{1}{1-\frac{\Sigma P_u}{\Sigma P_e}} = \frac{1}{1-\frac{214.4}{1702}} = 1.144 > 1 \text{ ok}$$

B2: At formation of second plastic hinge: The buckling load just after the formation of the second plastic hinge is shown in Fig. 8d, which leads to the following:

P_{cr} = 1167 kN

$$B2 = \frac{1}{1-\frac{\Sigma P_u}{\Sigma P_e}} = \frac{1}{1-\frac{214.4}{1167}} = 1.225 > 1 \text{ ok}$$

.

B2: At formation of third plastic hinge: The buckling load just after the formation of the third plastic hinge is shown in Fig. 8e, which leads to the following:

P_{cr} = 242 kN

$$B2 = \frac{1}{1-\frac{\Sigma P_u}{\Sigma P_e}} = \frac{1}{1-\frac{214.4}{242}} = 8.768 > 1 \text{ ok}$$

B2: At formation of fourth plastic hinge: The buckling load just after the formation of the fourth plastic hinge is zero. This is the formation of mechanism which leads to collapse state. In this case, B2, becomes infinite as the structure cannot support any additional loads.

The same procedures are repeated for the other load intensity cases. The resulting plastic magnification factor of all cases are shown in Table 8. Notice that if the external axial loads in the frame exceed the buckling load, B2, becomes negative indicating failure case. This state is shown in the table by dashed lines.

RESULTS AND DISCUSSION

The results of the previous analysis are compiled and analyzed in this section. Figure 9 shows comparison between the ultimate load resistance of the frame as each of the plastic hinges form from elastic stage to failure mechanism. Four mentioned methods of analysis, namely, first order elastic, second order elastic, first order plastic and second order plastic method are used to evaluate frame resistance. This comparison is made for axial load intensities P_u/P_y = 0.1 to 0.75. It should be pointed out that the elastic frame resistance stops just before the formation of the first plastic hinge. However, horizontal lines are drawn for the elastic cases for comparison purposes.

Examination of frame Fig. 9 shows that the frame strength decreases, in general, as the ratio of the axial load increases from 0.1 to 0.75. It can also be observed that while the frame strength increases as plastic hinges form in first order plastic analysis, the frame strength decreases as plastic hinges form in second order plastic analysis.

It can also be observed that, in all cases, the frame strength falls at or below the second order elastic strength at the formation of the first plastic hinge, which is something opposite to the notion that plastic design results in stronger structures and hence more economical ones.

In addition, Fig. 9 indicates that in all cases, the frame strength severely deteriorates before achieving the mechanism failure obtained by first order plastic analysis. It can also be observed that first order mechanism is reached for low axial load ratios, (0.1 and 0.2), while failure takes place before reaching this mechanism for moderate axial load ratios, (0.3 and 0.4) and for high axial load ratios, (0.6 to 0.75).

Figure 9 also indicates that for moderate and high axial load ratios, the frame collapses at the formation of the third plastic hinge formation according to second order plastic analysis, i.e., the frame collapses at earlier stage before the formation of the failure mechanism assumed to take place in first order plastic analysis.

It can also be observed in Fig. 9 that the frame strength in second order plastic analysis, which is a more realistic procedures, falls below its strength in second order elastic analysis. In fact, the second order plastic strength nearly matches the second order elastic strength and starts to deteriorate thereafter.

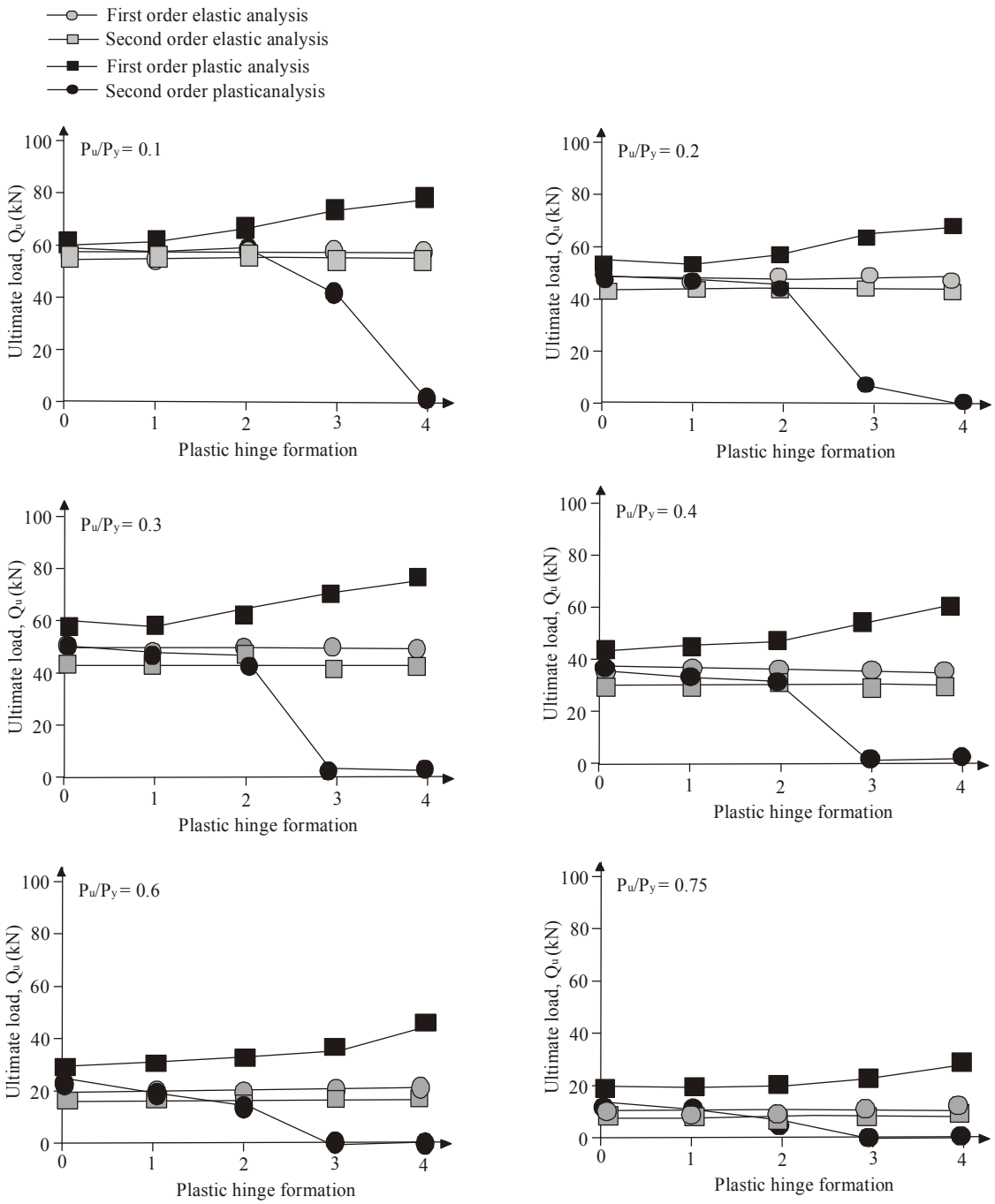

Fig. 9: Frame resistance load at formation of plastic hinges for various axial load intensities

Figure 10 and 11 further illustrate the relationship between first order plastic analysis, second order plastic analysis and the intensity of axial load in the structure. Figure 10a shows comparison between the strength of the frame in first order analysis at various axial load ratios, while Fig. 10b shows the frame strength in second order analysis at various load ratios. Figure 11 shows also comparison between the frame strength in first order plastic analysis and second order plastic analysis referenced to the frame strength just before the formation of the first plastic hinge.

It should be pointed out that, in first order plastic analysis, the frame strength, regardless of the axial load intensity, increases by the same ratio as plastic hinges form up to the formation of the plastic hinge before the last one, i.e., plastic hinge #3, as shown in Fig. 11a. Thereafter, the ratio of the mechanism strength starts to increase for higher axial load ratios.

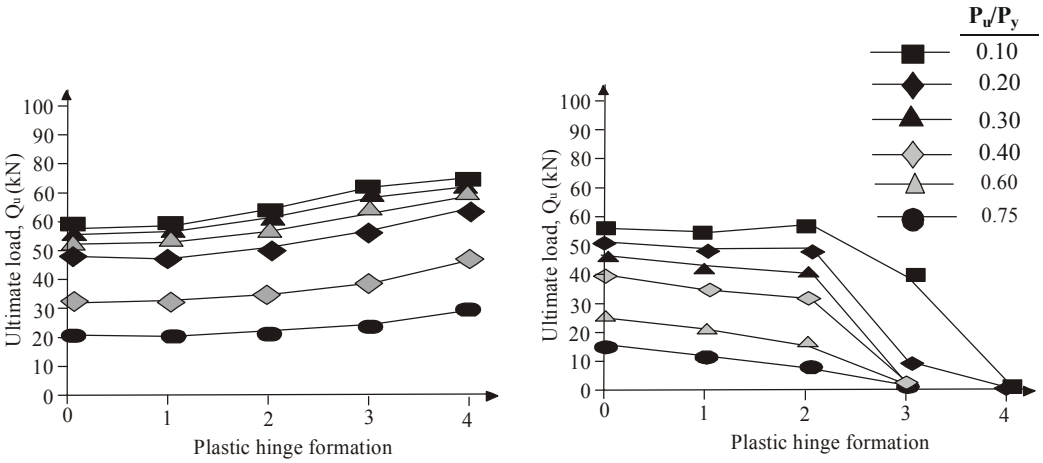

(a) First order plastic analysis (b) Second order plastic analysis

Fig. 10: Frame resistance load at formation of plastic hinges for various axial load intensities

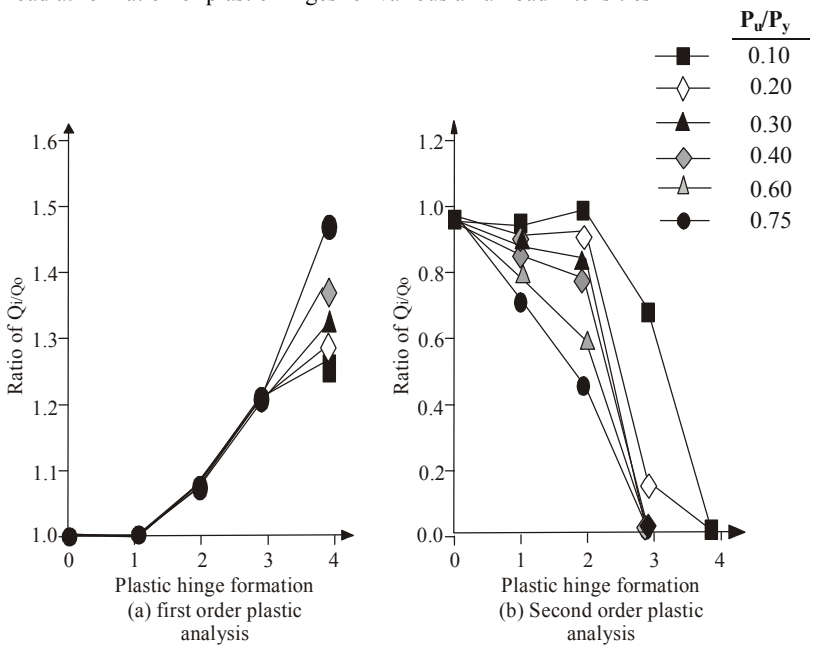

Fig. 11: Ratio of frame resistance load to the load just before formation of first plastic hinge

CONCLUSION

It can be concluded that second order plastic analysis must be utilized for analyzing steel frames as it results in frame strength much lower than first order plastic analysis and even more, lower than second order elastic analysis. The first order plastic analysis highly overestimates the actual strength of frames as it does not take into consideration the reduction of strength due to second order effect, P-Δ effect. It does not also take into consideration the effect of softening (formation of plastic hinges) on the stability of the structure, which in turn, on the P-Δ effect and on the resulting magnification of internal forces and moments.

It can also be concluded that the second order elastic analysis is more realistic than first order plastic analysis. In this study, it has been shown that the strength peak of the structure is reached just before the formation of the first plastic hinge where the strength starts to deteriorate thereafter. It is also shown that the structure reaches its failure limit state earlier before the development of the full failure mechanism, especially, for moderate and high axial loads in the structure.

It is obvious that the magnification factor, B2, that is currently used in AISC code is not valid for plastic analysis as it is based on elastic state of the structure, which is a state that does not exist after the formation of the first plastic hinge and therefore, the critical load calculated accordingly is not correct.

This study takes the opportunity to introduce simplified procedures to evaluate the second order effect based on plastic magnification factor, B2, taking

the inelastic buckling load into consideration by including the formation of plastic hinges in the process. These procedures definitely have the advantage over the lengthy and hectic finite element elasto-plastic procedures that proved to be overwhelming and unpopular in practical design environment.

The AISC, as one of the major codes recognized internationally, points out the importance of second order effect in plastic analysis; however, it does not give any details or guidelines on how to implement such analysis. Therefore, it is recommended that codes seek research to generalize guidelines on the inclusion of second order effect in plastic design in practical manner and if possible, produce clear practical procedures for conducting second order plastic analysis similar to second elastic analysis procedure case.

REFERENCES

ACI, 2011. Building code requirements for Structural Concrete (318M-11). American Concrete Institute, Farmington Hills, MI 48331, pp: 503.

AISC, 2010. Specification for Structural Steel Buildings. American Institute of Steel Construction, Chicago, IL 60601.

Alvarenga, A.R. and R.A.M. Silveira, 2009a. Second-order plastic-zone analysis of steel frames, Part I: Numerical formulation and examples of validation. Lat. Am. J. Solids Stru., 6: 131-152.

Alvarenga, A.R. and R.A.M. Silveira, 2009b. Second-order plastic-zone analysis of steel frames, Part II: Effects of initial geometric imperfection and residual stress. Lat. Am. J. Solids Stru., 6: 323-342.

Beedle, L.S., 1958. Plastic Design of Steel Frames. John Wiley and Sons, New York.

Bi, J.H., R. Cong and L.H. Zhang, 2004. Elastoplastic and large deflection analysis of steel frames by one element per member, Part 1 and 2. J. Struct. Eng., 130(4): 538-553.

Chan, S.L. and Z.H. Zhou, 2004. Elastoplastic and large deflection analysis of steel frames by one element per member, Parts 1 and 2. J. Struct. Eng., 130(4): 538-553.

Chen, W.F. and D.J. Han, 1988. Plasticity for Structural Engineers. Berlin: Springer, New York.

Chen, W.F. and E.M. Lui, 1987. Structural Stability: Theory and Implementation. Elsevier, New York.

Chen, W.F. and I.S. Sohal, 1995. Plastic Design and Second-Order Analysis of Steel Frames. Spring-Verlag, New York.

Mesic, E., 2007. Plasticization process of steel frames through discretization of plastic zone. Archit. Civ. Eng. Facta Univ., 5(2): 87-94.

Trahair, N.S., 2012. Trends in the analysis and design of steel framed structures. School of Civil Engineering, The University of Sydney, Australia, Research Report No R926.

Wong, M.B., 2009. Plastic Analysis and Design of Steel Structures. 1st Edn., Butterworth-Heinemann, Amsterdam, Boston.